LIMNOLOGY
and
OCEANOGRAPHY

ASLO

Limnol. Oceanogr. 00, 2017, 00–00
© 2017 The Authors Limnology and Oceanography published by Wiley Periodicals, Inc.
on behalf of Association for the Sciences of Limnology and Oceanography
doi: 10.1002/lno.10625

Limitation of dimethylsulfoniopropionate synthesis at high irradiance in natural phytoplankton communities of the Tropical Atlantic

Stephen D. Archer,[1]* **Jacqueline Stefels**,[2] **Ruth L. Airs**,[3] **Tracy Lawson**,[4] **Timothy J. Smyth**,[3] **Andrew P. Rees**,[3] **Richard J. Geider**[4]

[1]Bigelow Laboratory for Ocean Sciences, East Boothbay, Maine
[2]Ecophysiology of Plants, Groningen Institute for Evolutionary Life Sciences, University of Groningen, Groningen, The Netherlands
[3]Plymouth Marine Laboratory, Plymouth, Devon, United Kingdom
[4]School of Biological Sciences, University of Essex, Colchester, Essex, United Kingdom

Abstract

Predictions of the ocean-atmosphere flux of dimethyl sulfide will be improved by understanding what controls seasonal and regional variations in dimethylsulfoniopropionate (DMSP) production. To investigate the influence of high levels of irradiance including ultraviolet radiation (UVR), on DMSP synthesis rates (μDMSP) and inorganic carbon fixation (μPOC) by natural phytoplankton communities, nine experiments were carried out at different locations in the low nutrient, high light environment of the northeastern Tropical Atlantic. Rates of μDMSP and μPOC were determined by measuring the incorporation of inorganic ^{13}C into DMSP and particulate organic carbon. Based on measurements over discrete time intervals during the day, a unique μDMSP vs. irradiance (P vs. E) relationship was established. Comparison is made with the P vs. E relationship for μPOC, indicating that light saturation of μDMSP occurs at similar irradiance to μPOC and is closely coupled to carbon fixation on a diel basis. Photoinhibition during the middle of the day was exacerbated by exposure to UVR, causing an additional 55–60% inhibition of both μDMSP and μPOC at the highest light levels. In addition, decreased production of DMSP in response to UVR-induced photoxidative stress, contrasted with the increased net synthesis of photoprotective xanthophyll pigments. Together these results indicate that DMSP production by phytoplankton in the tropical ocean is not regulated in the short term by the necessity to control increasing photooxidative stress as irradiance increases during the day. The study provides new insight into the regulation of resource allocation into this biogeochemically important, multi-functional compatible solute.

The oceans emit approximately 28.1 (17.6–34.4) million tons of sulfur in the form of dimethyl sulfide (DMS) each year (Lana et al. 2011), representing the largest natural flux of sulfur to the atmosphere. DMS is a product of the enzymatic breakdown of β-dimethylsulfoniopropionate (DMSP), an osmolyte synthesized by phytoplankton (Challenger and Simpson 1948). In recent years, the debate has intensified over the original proposal that DMS emission from the oceans contributed to an oceanic biology—climate feedback loop (Charlson et al. 1987; Cainey et al. 2008; Woodhouse et al. 2010; Quinn and Bates 2011). Nonetheless, this considerable source of sulfur has a substantial impact on atmospheric chemistry (Toumi 1994; Johnson and Bell 2008; Chen and Jang 2012). Oxidation of DMS results in the formation of sulfuric acid (H_2SO_4) and methylsulfonic acid (MSA). Sulfuric acid is the primary vapor responsible for new aerosol particles and cloud condensation nuclei (Sipilä et al. 2010; Kirkby et al. 2011), while MSA often makes a major contribution to the growth of existing aerosols (Rinaldi et al. 2010). Incorporation of the global seawater DMS climatology (Lana et al. 2011) into an aerosol-chemistry-climate general circulation model, illustrates large regional and seasonal variations in the cooling effect of DMS of ± 10 W m^{-2} and a global mean annual influence of close to -2.0 W m^{-2} (Mahajan et al. 2015). The magnitude of change in DMS emissions in the future remains an important issue for global atmospheric chemistry and climate.

Mechanistic models that relate DMS emissions from the oceans to DMSP production and cycling, have attempted to capture the taxonomic and physiological factors that

*Correspondence: sarcher@bigelow.org

This is an open access article under the terms of the Creative Commons Attribution License, which permits use, distribution and reproduction in any medium, provided the original work is properly cited.

influence DMSP production to varying degrees (reviewed in Le Clainche et al. 2010). However, the competitive advantage DMSP production confers and how this contributes to temporal and regional patterns in production of DMS, remains unclear. Phytoplankton have generally been represented by between two and four functional types that differ in their DMSP cell quota (e.g., DMSP : carbon ratio) based largely on information derived from laboratory cultures of different microalgal strains (reviewed in Stefels et al. 2007). Intracellular concentrations vary between species of microalgae from undetectable levels to 100s mmol L^{-1} (Keller et al. 1989). Modeled DMSP production is then a product of the DMSP cell quota, succession of the phytoplankton functional types, and primary production. In several models, parameterization of DMSP cell quotas has included the influence of light and/or nutrient availability and temperature dependence (e.g., Vallina et al. 2008; Vogt et al. 2010; Polimene et al. 2012), reflecting possible physiological roles of DMSP.

DMSP appears to play multiple, potentially simultaneous roles in microalgae (reviewed in Stefels 2000, Stefels et al. 2007). The potential for accumulation of DMSP in the chloroplasts of microalgae (Lyon et al. 2011) and demonstrated chloroplast localization in higher plants (Trossat et al. 1998) supports the theory that DMSP, and possibly its breakdown products, may protect photosynthetic systems from oxidative damage caused by excess irradiance or nutrient limitation (Sunda et al. 2002). In contrast, a metabolic overflow hypothesis proposes that DMSP is synthesized to regulate intracellular methionine concentrations and photosynthetic overcapacity during unbalanced growth resulting from excess irradiance or nutrient limitation (Stefels 2000). DMSP may be employed as a methyl donor in biological transmethylation reactions (Ishida 1996 and references therein) and may be a precursor in the biosynthesis of the membrane phospholipid phosphatidylsulphocholine in marine microalgae (Kates and Volcani 1996). In addition, DMSP has been proposed to have a role as a grazing deterrent when ingestion or digestion of phytoplankton by grazers results in its enzymatic cleavage to DMS and acrylate (Dacey and Wakeham 1986; Wolfe and Steinke 1996), although DMSP has also been shown to be a chemoattractant for a variety of planktonic microbes (Seymour et al. 2010). Successfully modeling DMSP production in the ocean may require understanding how the environment affects which physiological roles drive synthesis and the cost vs. benefits of resource allocation to produce DMSP.

There is a growing appreciation of the benefits in understanding photosynthetic resource allocation in phytoplankton in order to explain elemental and energetic stoichiometry and their impacts on community structure and ecosystem productivity (reviewed in Halsey and Jones 2015). This study expands this theme to how resource allocation by phytoplankton has implications for the atmosphere-ocean exchange of trace gases that influence atmospheric chemistry. Understanding how physiology and environmental variables affect the allocation of resources to metabolic pathways that result in the production of these volatile products may improve the capability of mechanistic models aimed at predicting ocean-atmosphere exchange rates. One of the hurdles to understanding what drives the allocation of resources to DMSP production, and how rapidly DMSP is transformed, is the lack of direct estimates of DMSP synthesis rates. The introduction of a stable-isotope approach to determine in vivo DMSP production rates enables us to investigate how environmental factors drive DMSP production in natural and culture-based systems (Stefels et al. 2009). Without this key measurement, it has proven challenging to link DMS production to DMSP physiological function.

Phytoplankton DMSP content and the rates at which it turns over, meaning synthesis vs. metabolism and release from cells, are key underlying factors that influence the seasonal and regional patterns of DMS in the ocean. This study investigated DMSP synthesis rates by natural phytoplankton communities in the high light, low nutrient environment of the subtropical and Tropical Atlantic Ocean. The resource allocation to DMSP was investigated by comparing directly measured rates of DMSP synthesis to rates of carbon fixation. The study aimed to also understand the physiological role of DMSP production by examining the influence of diel patterns of exposure to photosynthetically active radiation (PAR) and ultraviolet radiation (UVR) and the consequence of high light-induced photooxidative stress on DMSP synthesis compared to carbon fixation. The response of DMSP synthesis to photooxidative stress was also compared to the synthesis of pigments involved in the xanthophyll cycle, an established photoprotective mechanism. The study is an advance on previous assessments of the physiological role of DMSP because it examines specific rates of DMSP synthesis in relation to phytoplankton physiology and environmental factors, as opposed to examining net changes in DMSP concentration. By doing so, the study provides a more direct assessment of DMSP function that is less influenced by the many processes that control concentrations of DMSP in natural planktonic communities.

Methods

Study area and experimental set-up

The experiments were conducted aboard the *RRS Discovery*, during cruise D326, in the northeastern Tropical Atlantic (12.5–26.6° N and 23.7–35.8° W) at nine different locations between 15th January 2008 and 2nd February 2008 (Fig. 1; Table 1). On each experimental date, a single 96 L volume of seawater was collected pre-dawn from twelve 10-liter Niskin bottles closed simultaneously at 5–8 m depth. The seawater was transferred gently and in the dark to 2 L, UVR-transparent, Whirl-pak® bags and incubated at in situ temperatures for the full daylight period in one of two flow-through incubators to which different natural light treatments were applied.

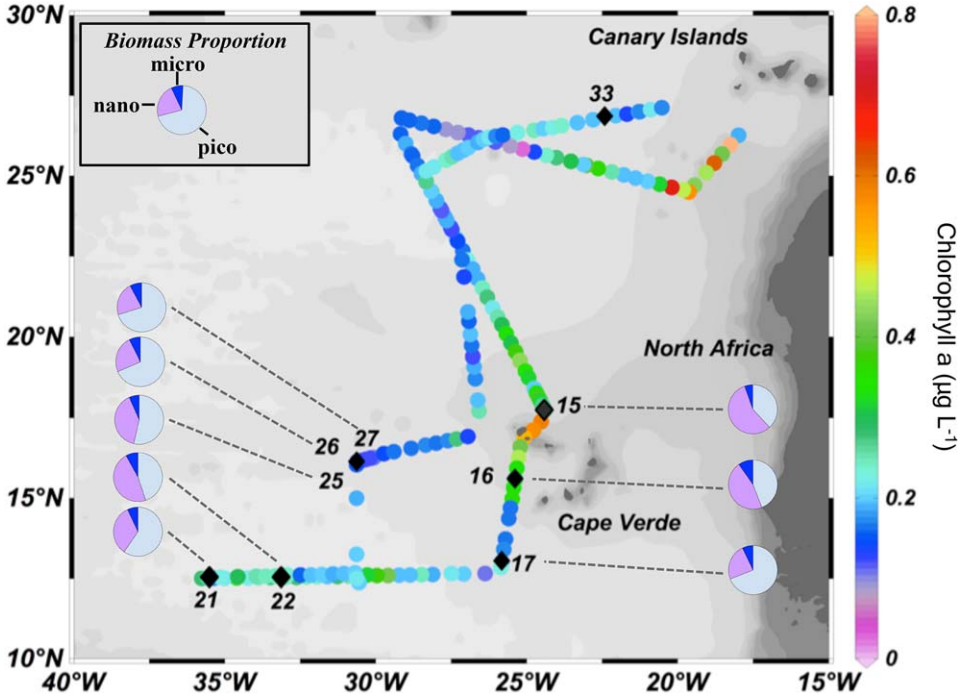

Fig. 1. Ocean Data View (Schlitzer 2015) chart of the D326 cruise track. The cruise started and finished in Tenerife, Canary Islands. The dots show Chl *a* (μg L^{-1}) concentrations measured from the underway water supply ($\sim$ 5 m depth). Stations from which experiments are reported (Table 1) are shown as black diamonds; the station numbers refer to day of the year. Biomass Proportion refers to an estimate of the proportion of total phytoplankton biomass composed of picoplankton, nanoplankton, and microplankton based on diagnostic pigment concentrations for each size class (Vidussi et al. 2001). No diagnostic pigment data was available for day 33.

Natural planktonic communities were exposed to two light treatments, one consisting of the full light spectrum of PAR+UV and a second PAR-UV treatment in which the UV was removed. A UV radiometer (UV-507) and a multispectral visible radiometer (OCI-200) (SAtlantic, Halifax, Nova Scotia, Canada) were used to monitor incoming irradiance at 305 nm, 325 nm, 340 nm, and 380 nm, and 411 nm, 442 nm, 490 nm, 510 nm, 620 nm, 665 nm, and 683 nm, respectively. These were integrated to calculate ultraviolet B (UVB), ultraviolet A (UVA), UVR (UVA + UVB), and PAR during incubations. Perspex® screens were used to remove UVR in one of the two sets of incubations and open-weave plastic mesh was used to adjust total levels of irradiance. In order to incorporate attenuation by the polyethylene Whirl-pak® bags, the radiometers were located immediately below the layer of bags during incubations. The PAR-UV incubations received 41–96% PAR; 7–36% UVA, and $<$ 0.05% UVB present in the full spectrum, PAR+UV treatment. At each of five time points during the approximately 12 h incubations, whole 2 L bags were removed and sub-sampled for a suite of measurements.

Photophysiological measurements

Variable fluorescence measurements were performed to quantify the influence of incubation light treatments on the extent of photoinhibition (Ragni et al. 2008). A fluorescence induction and relaxation (FIRe) fluorometer (SAtlantic, Halifax, Nova Scotia, Canada) was used to acquire discrete measurements in samples adapted to the dark for $>$30 min, to ensure that modifications in photophysiology were a result of photoinhibition rather than nonphotochemical quenching (NPQ). Three mL samples in a cylindrical 1 cm path length cuvette were placed into the FIRe fluorometer. At each time point, samples from three separate 2 L bags were analyzed for each treatment. Excitation was provided by a high luminosity blue and green LED array (450 nm and 500 nm peak heights). The two-step protocol consisted of (1) single turnover (ST) excitation from a 100 μs pulse, and (2) ST relaxation from a weak modulated light over 500 ms. Blank measurements were performed on 0.2 μm filtered seawater. The biophysical model of Kolber et al. (1998) was applied to fit the data using the software FIREPRO (v.1.20, Satlantic). The retrieved parameters used in this study are the minimum (F_0) and maximum (F_m) fluorescence yields and the maximum photochemical efficiency of photosystem II (PSII) (F_v/F_m). The net rate of photoinhibition (NPiR) was calculated from the rate of decrease in F_v/F_m (Ragni et al. 2008).

Quantification of DMS and DMSP concentrations

At each time point, samples from two or three separate 2 L bags were analyzed immediately for DMS and preserved for DMSP analysis. For DMS concentrations, 10 mL samples

Table 1. Sample times and depths and initial characteristics of the water used for the nine experiments. DMSPt refers to total DMSP concentration, largely composed of particulate DMSP but includes a small (generally < 5%) component of dissolved DMSP. Chl *a* is chlorophyll *a* and Dd + Dt is the combined concentration of xanthophyll pigments diadinoxanthin (Dd) and diatoxanthin (Dt). Concentrations are the average of duplicate samples from the water collected for the experimental incubations. nd, no data.

Date (day of year)	Depth (m)	Time	Water temp (°C)	DMS (nmol L^{-1})	DMSPt (nmol L^{-1})	Chl *a* (μg L^{-1})	Dd+Dt (ng L^{-1})	DMSP : Chl *a* (nmol μg^{-1})
15 Jan 2008 (15)	8	05:36	22.3	1.2	21	0.28	13.0	75
16 Jan 2008 (16)	8	05:41	23.1	1.4	15	0.34	9.8	44
17 Jan 2008 (17)	8	05:40	24.5	1.5	12	0.21	5.4	57
21 Jan 2008 (21)	7	05:40	24.9	1.4	10	0.20	6.1	50
22 Jan 2008 (22)	8	05:42	24.6	0.8	10	0.19	4.2	53
25 Jan 2008 (25)	8	05:43	23.5	0.7	13	0.14	4.9	93
26 Jan 2008 (26)	7	05:40	23.4	nd	12	0.13	4.2	92
27 Jan 2008 (27)	6	05:40	23.4	1.2	11	0.13	3.8	85
02 Feb 2008 (33)	6	06:34	21.0	0.5	8	0.21	nd	38

from a 2 L bag were gently filtered through a GF/F filter prior to injection into the purge system. For determination of total DMSP (DMSPt) concentrations, which includes particulate DMSP (DMSPp) and a minor dissolved DMSP (DMSPd) fraction, samples were fixed by addition of 35 μL of 50% H_2SO_4 to 7 mL of seawater (Kiene and Slezak 2006). This procedure oxidizes > 98% of any DMS present in the sample to nonvolatile products within 24 h (Kiene and Slezak 2006). Samples for DMSPt were analyzed at Plymouth Marine Laboratory, several months after the cruise. The samples were hydrolyzed for > 6 h with a pellet of NaOH to convert DMSP to DMS. Two milliliter of the sample was then transferred, with care taken to minimize gas exchange, to a glass purge tower for extraction of DMS. Calibration for DMS in seawater used 10–100 μL additions of a DMS standard dissolved in methanol to 10 mL of MilliQ water. Standard DMS concentrations covered a range equivalent to 0.2–2.0 nmol L^{-1}. Calibration for DMSPt used the same DMS standards in 2 mL purge volumes covering a range of concentrations equivalent to 7–70 nmol L^{-1}.

DMS concentrations were measured using a purge system and liquid-nitrogen cryogenic trap linked to a Varian 3800 gas chromatograph equipped with a pulsed flame photometric detector and Varian 30 m × 0.53 mm CP Sil 5CB column (Archer et al. 2013). When triplicate experimental samples were used to test for analytical error, standard deviation was typically < 10% of the mean for both DMS and DMSPt.

Quantification of phytoplankton pigment concentrations

Pigment concentration and composition, in particular that of the photoprotective xanthophyll pigments diadinoxanthin (Dd) and diatoxanthin (Dt), were determined at three time-points during the incubation experiments (0 h, ~ 6 h, and ~ 12 h). For each measurement, two bags were used to obtain a 4 L sample from the incubations, that was filtered onto 47 mm GF/F filters, flash frozen in liquid nitrogen and stored at −80°C until analyzed.

Pigments were extracted from GF/F filters into 2 mL of 100% acetone containing an internal standard (apocarotenoate; Sigma, Poole, Dorset, UK) using an ultrasonic probe (30 s, 50 W). Extracts were centrifuged to remove filter and cell debris (5 min at 2000 g) and analyzed by HPLC using a reversed-phase C8 column and gradient elution (Barlow et al. 1997) on an Agilent 1100 Series high performance liquid chromatograph (HPLC) system with chilled autosampler and photodiode array detection (Agilent Technologies, South Queensferry, West Lothian, UK). The HPLC was calibrated using a suite of standards (Danish Hydraulic Institute, Denmark) and pigments identified in the samples from retention time and spectral match (Jeffrey et al. 1997).

Determination of phytoplankton abundance

At each station, the initial nano- and picophytoplankton composition and abundance were determined in the incubation water by analysis of fresh samples on a Becton Dickinson FACSort flow cytometer equipped with a 15 mW laser exciting at 488 nm and with a standard filter set up. The flow rate was calculated by adding known concentrations of 0.5 μm yellow-green fluorescent latex beads (Polysciences, Eppelheim, Germany) as an internal standard (Zubkov and Burkill 2006). Specific phytoplankton groups were discriminated in bivariate scatter plots by differences in side scatter and red-orange fluorescence, using CellQuest software (Becton Dickinson, Oxford, UK).

DMSP synthesis rates

De novo DMSP synthesis rate (μDMSP) was determined from the rate of incorporation of dissolved inorganic ^{13}C into DMSPp (Stefels et al. 2009). Trace (< 2% of in situ dissolved inorganic carbon [DIC]) stable isotope concentrations were added to the 96 L volume of seawater before it was dispensed into the Whirl-Pak® bags. The exact tracer addition

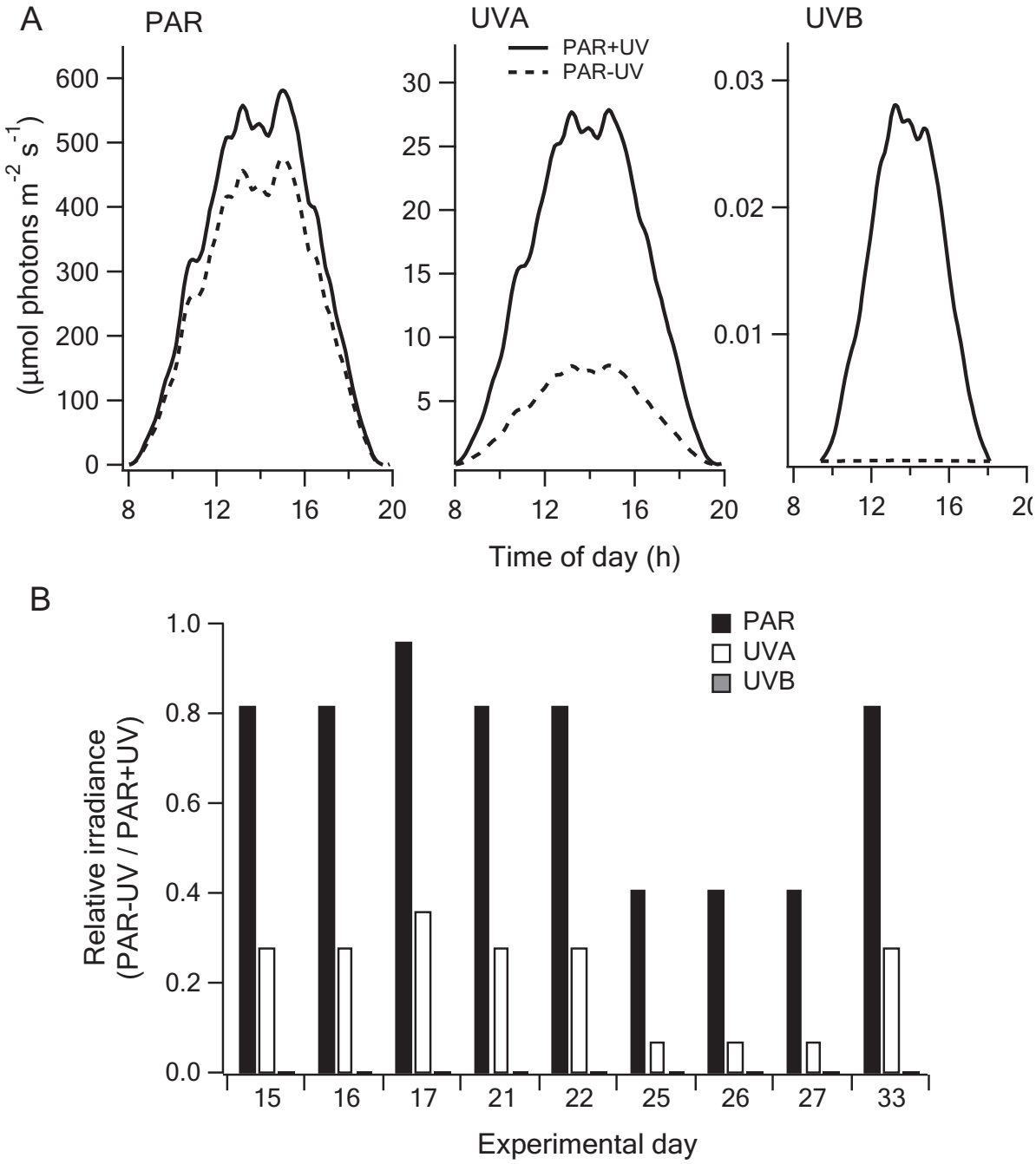

Fig. 2. Irradiance measured in the incubation tanks (**A**) for the experiment on 15th January 2008, illustrating the substantially higher UVA and UVB experienced by the phytoplankton in PAR+UV compared to PAR-UV treatments. The lines connect 5 min averaged measurements. (**B**) Relative irradiance levels of PAR, UVA, and UVB in PAR-UV treatments compared to PAR+UV (PAR-UV/PAR+UV) during each of the experiments.

was subsequently calculated from the weight of $NaH^{13}CO_3$ added and daily measurements of in situ DIC concentration measured in water collected at the same depth and time as the 96 L used for the incubation experiments. At 4 or 5 time points during the ~ 12 h incubations, duplicate 1 L volumes from each treatment were gravity filtered in the dark onto a 47 mm GF/F filter. Filters were placed in a 20 mL crimp-cap vial to which 10 mL of 0.5 M NaOH was added. For storage, the samples were frozen at −20°C.

Incorporation of ^{13}C into DMSP was determined by proton-transfer-reaction mass spectrometry (PTR-MS, Ionicon GmbH, Innsbruck, Austria) of DMS swept from the 20 mL vials and recorded as mass 63, 64, and 65 of protonated forms of ^{12}C-DMS, ^{13}C-DMS, ^{34}S-DMS, respectively. The masses from 30

Table 2. Light levels in the flow-through incubators and in the water column at each station. The attenuation coefficient of PAR (K_d) was determined from linear regression of the natural logarithm of downwelling irradiance vs. depth. Mixed layer depth (MLD) was determined as the depth of a 0.1°C change in temperature from the surface value. The photoactive depth for UVR, Z10% 320 nm, was calculated from K_d 320 nm (Z10% = 2.3/K_d) (Tedetti and Sempéré 2006). Comparison of the average light levels in the incubations, through the mixed layer and in the upper 10 m of the water column are shown as percentages of the irradiance just below the surface.

	Day of the year								
	15	16	17	21	22	25	26	27	33
PAR+UV treatment daily integral (mol photons m^{-2} d^{-1})									
PAR	12.7	15.9	11.8	23.0	26.0	20.1	22.1	22.0	9.6
UVA	0.62	0.73	0.45	1.09	1.20	0.89	0.95	0.94	0.62
UVB	0.020	0.045	0.024	0.064	0.070	0.050	0.054	0.054	0.034
In situ light environment									
K_d PAR (m^{-1})	−0.067	−0.079	−0.058	−0.049	−0.062	−0.052	−0.030	−0.049	−0.038
MLD (m)	69	38	48	68	60	39	34	68	146
Photoactive zone (Z10% 320 nm) (m)	21	19	25	24	24	25	36	32	25
Daily integral as % of surface irradiance									
PAR+UV incubation	81	79	69	86	83	85	91	86	86
Mixed layer average	20	33	36	27	29	46	57	49	14
Upper 10 m average	70	73	82	83	81	86	77	80	85

data points, at a 1 s dwell interval, of the peak of the DMS signal were used to calculate the mass ratio of 1 × ^{13}C-DMSP (^{64}MP) at each point. A weighted average approach that gives most weight to the initial points of the exponentially decreasing DMS peak was used to calculate the mass ratio $^{64}MP_t$ for each sample at each time point. The mass ratio progress method described by Stefels et al. (2009) was applied to calculate μDMSP. To account for uncertainty due to isotope-fractionation, the isotope fractionation factor from culture-based studies of *Emiliania huxleyi* was applied (Stefels et al. 2009). By incorporating shorter time intervals of ≤ 6 h within the ~ 12 h incubations, uncertainty associated with turnover of the DMSP pool is reduced, ensuring that the μDMSP measurement is close to the gross synthesis rate. DMSP production was calculated from the initial DMSPt concentration, measured by purge-and-trap gas chromatography, and μDMSP. This assumes that the isotope fraction is not different between DMSPt, which includes a minor dissolved component, and the particulate DMSP sample analyzed by PTR-MS, the filtration of which may have caused loss of a portion of the particulate component.

Carbon fixation rates

Inorganic carbon fixation (μPOC) was determined from the incorporation of ^{13}C, added as $NaH^{13}CO_3$, into particulate organic carbon (POC). From the same incubation bags used for determination of μDMSP, duplicate 1 L samples were filtered using < 5 mm Hg vacuum, onto 25 mm GF/F filters, rinsed with unlabeled, filtered seawater, flash frozen in liquid nitrogen and stored at −80°C until analyzed. On return to the laboratory, filters were acid fumed, dried overnight at 50°C and analyzed for POC concentration and the ratios of $^{13}CO_2$ to $^{12}CO_2$ (mass 45/44) by continuous flow analysis-mass spectrometry using a PDZ Europa ANCA-GSL elemental analyser interfaced to a PDZ Europa 20–20 isotope ratio mass spectrometer (Sercon, Cheshire, UK). The mass ratio progress method described by Stefels et al. (2009) was applied to calculate μPOC.

Results

Experimental setting

The experiments were conducted using waters that varied threefold in initial chlorophyll *a* concentration from 0.13 μg L^{-1} to 0.34 μg L^{-1}, typical of the northeastern Tropical Atlantic (Fig. 1; Table 1). Based on diagnostic pigment concentrations (Vidussi et al. 2001), the phytoplankton communities were dominated by picoplankton and nanoplankton, with microplankton making up an estimated < 10% of the total biomass (Table 1; Fig. 1). Initial abundances of nanophytoplankton in the experimental water ranged from 2.7 × 10^6 cells L^{-1} at more westerly stations, to 7.7 × 10^6 cells L^{-1} in proximity to Cape Verde. Picoeukaryote and *Synechococcus* abundance showed a similar distribution pattern and varied in abundance from 0.4 × 10^6 cells L^{-1} to 2.7 × 10^6 cells L^{-1} and 4 × 10^6 cells L^{-1} to 54 × 10^6 cells L^{-1}, respectively. In contrast, the abundance of *Prochlorococcus* was highest in lower Chl *a* waters to the south and west of Cape Verde, varying from 74 × 10^6 cells L^{-1} to 210 × 10^6 cells L^{-1}.

Initial DMSPt concentrations were 8–21 nmol L^{-1}, with an average DMSPt : Chl *a* ratio of 65 (range 38–93) nmol μg^{-1} amongst the stations (Table 1) indicating moderately

DMSP-rich phytoplankton communities. In a global context, a median value of 99 nmol μg^{-1} was calculated from the Global Surface Seawater DMS database (http://saga.pmel.noaa.gov/dms/) that includes ~ 4600 measurements of DMSPt (Galí and Simó 2015). DMS concentrations varied between 0.5 nmol L^{-1} and 1.5 nmol L^{-1} (Table 1), consistent with the low DMS values reported for January and February in the climatology compiled for the North Atlantic Tropical Gyral Province (Lana et al. 2011).

Light during incubations followed a typical diel pattern in near-surface waters (Fig. 2A). The daily integrals of PAR, UVA, and UVB in the PAR+UV treatments varied more than twofold between experiments as a result of differences in daily irradiance and the mesh screens used in some of the experiments (Table 2). The varied amounts of mesh used in the experiments attenuated solar radiation in the PAR+UV treatment by 62–100% for PAR, 51–100% for UVA, and 47–100% for UVB. The PAR+UV treatments received PAR at levels equivalent to 69–91% of the light immediately below the surface. This was generally approximately double the average level of downwelling irradiance in the mixed layer of the related water column but comparable to average light levels in the upper 10 m (Table 2). The PAR-UV incubations received 41–96% of PAR; 7–36% of UVA, and < 0.05% of UVB present in the PAR+UV treatment (Fig. 2B). The depth of UVR penetration in the water column, the photoactive zone (Z10% 320 nm), varied between 19 m and 36 m at the experimental stations (Table 2).

Photophysiological response

Initial values of F_v/F_m in dark-adapted samples ranged from an average of 0.49–0.56 in the nine experiments. All the phytoplankton communities exhibited increased photoinhibition during the middle of the day, evident as a decrease in F_v/F_m, as shown for the experiment on day 26 (Fig. 3). This is typical of phytoplankton populations in low nutrient, low biomass open ocean environments (e.g., Mackey et al. 2008). In all experiments, F_v/F_m recovered to close to initial values by the end of the incubations (Fig. 3), indicating that the phytoplankton communities were able to employ effective photoprotective strategies to prevent permanent damage to photosystems. The levels of photoinhibition (NPiR) were typically higher in PAR+UV than in PAR-UV treatments (Fig. 3B).

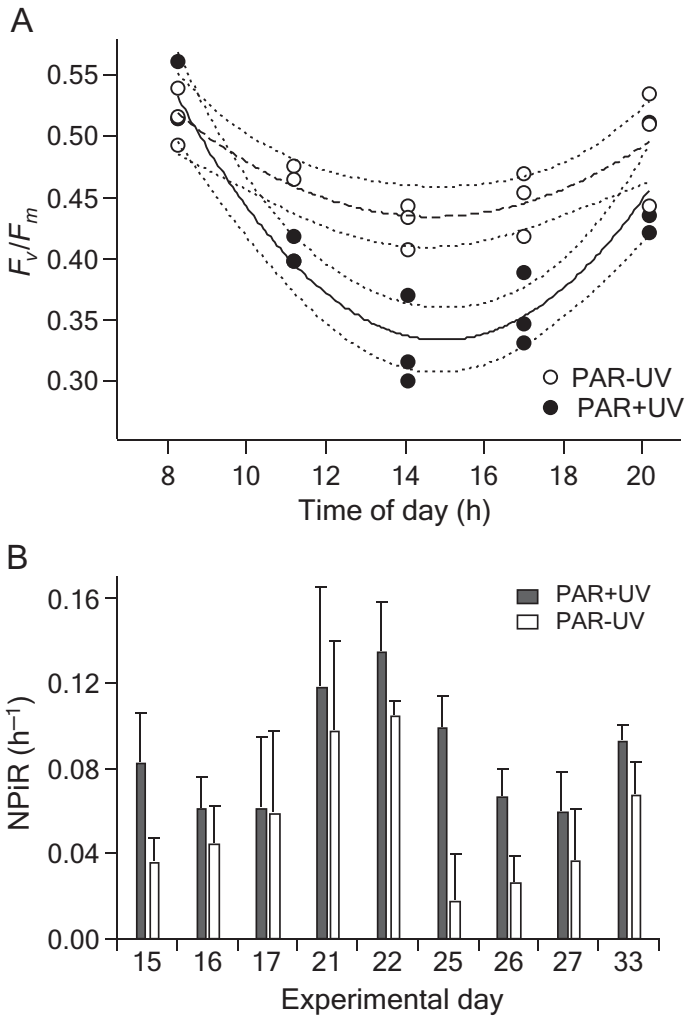

Fig. 3. Photophysiological response to the incubation treatments. (**A**) Change in maximum photochemical efficiency (F_v/F_m) during the experiment on 26th January 2008 for PAR+UV and PAR-UV treatments. Dotted lines show the 95% confidence intervals for the fitted polynomial curves. For each light treatment, NPiR was calculated from the fitted curve from values for the initial F_v/F_m ($F_v/F_{m(T0)}$) and minimum F_v/F_m ($F_v/F_{m(T\min)}$) [NPiR = −Ln ($F_v/F_{m(T\min)}/F_v/F_{m(T0)}$)/($T_{\min} - T_0$)], In this case, values of NPiR were 0.067 h^{-1} and 0.027 h^{-1} for PAR+UV and PAR-UV treatments, respectively. (**B**) Rates of NPiR in PAR+UV and PAR-UV treatments for each experiment. The uncertainty in NPiR was calculated from the upper 95% $F_v/F_{m(T0)}$ value to the lower 95% $F_v/F_{m(T\min)}$ value and vice versa, illustrated in (**A**).

DMSP synthesis and carbon fixation

An example of the incorporation rate of ^{13}C into DMSP during the incubations on day 26 is shown in Fig. 4A. Specific DMSP synthesis rates [μDMSP (h^{-1})] were determined for each of the time intervals (Fig. 4C) and can be integrated to determine a daily rate over the full incubation period. For instance on day 26, this gave a daily μDMSP rate (± SD) of 0.22 ± 0.03 d^{-1} and 0.21 ± 0.04 d^{-1} for PAR-UV and PAR+UV treatments, respectively (Table 3). This daily rate assumes no incorporation of ^{13}C into DMSP in the dark. From the same incubations, the rate of ^{13}C incorporation into POC is illustrated in Fig. 4B, from which a specific rate of POC synthesis [μPOC (h^{-1})] was obtained (Fig. 4D). Corresponding daily rates of μPOC were 0.029 ± 0.009 d^{-1} and 0.032 ± 0.008 d^{-1} for PAR-UV and PAR+UV treatments, respectively (Table 3).

For the six stations at which μPOC was determined, daily rates from the PAR+UV incubations were significantly related to Chl *a* concentration (Fig. 5A). An even more significant relationship, in part due to the greater number of

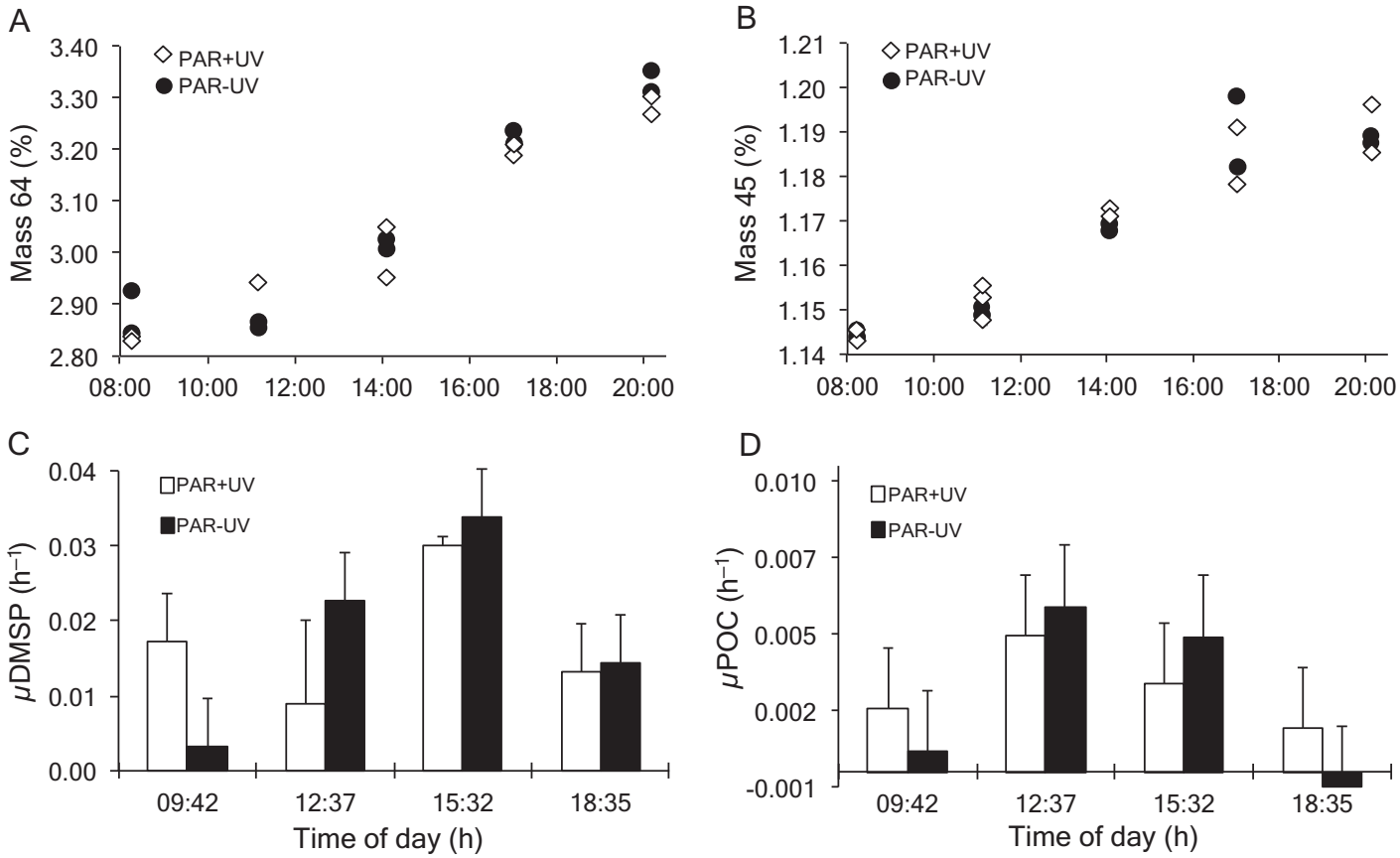

Fig. 4. DMSP and POC specific synthesis rates on 26th January in parallel incubations under PAR+UV and PAR-UV irradiance. (**A**) Incorporation of ^{13}C into DMSP quantified as the percentage of DMS of mass 64/(mass 63 + mass64 + mass 65); (**B**) incorporation of ^{13}C into POC expressed as the percentage of CO_2 mass 45/(mass 44 + mass 45); (**C**) specific synthesis rate of DMSP (μDMSP); and (**D**) specific rate of incorporation of inorganic carbon into POC (μPOC) during each incubation time interval. Times shown in (**C**) and (**D**) are the mid-point of each incubation period. Bars are the SD.

Table 3. Daily values of μDMSP and μPOC and estimates of daily production. Daily values were calculated from integrated μDMSP and μPOC for each time interval over the $\sim$ 12 h incubations. Errors are the propagated SD. Production rates were calculated from the initial DMSPt or POC value on each day and daily μDMSP and μPOC. nd, no data.

	μDMSP		μPOC				
Experiment (DoY)	**PAR-UV (d^{-1})**	**PAR+UV (d^{-1})**	**PAR-UV (d^{-1})**	**PAR+UV (d^{-1})**	**DMSP production PAR+UV (nmol L^{-1} d^{-1})**	**Carbon fixation PAR+UV (μg C L^{-1} d^{-1})**	**Proportion of DMSP production (% carbon fixation)**
15	0.28 ± 0.01	0.29 ± 0.02	nd	nd	7.0	nd	nd
16	0.45 ± 0.07	0.38 ± 0.05	nd	nd	7.5	nd	nd
17	0.31 ± 0.01	0.24 ± 0.05	nd	nd	3.2	nd	nd
21	0.32 ± 0.03	0.23 ± 0.05	0.052 ± 0.004	0.049 ± 0.005	3.7	3.8	5.8
22	0.31 ± 0.11	0.20 ± 0.09	0.082 ± 0.005	0.044 ± 0.006	3.0	3.4	5.2
25	0.21 ± 0.05	0.15 ± 0.03	0.043 ± 0.008	0.030 ± 0.005	2.9	2.4	7.3
26	0.22 ± 0.03	0.21 ± 0.04	0.029 ± 0.009	0.032 ± 0.008	3.9	2.4	9.7
27	0.19 ± 0.05	0.22 ± 0.08	0.041 ± 0.009	0.037 ± 0.007	3.4	2.9	6.8
33	0.22 ± 0.02	0.20 ± 0.05	0.036 ± 0.004	0.043 ± 0.005	2.5	3.5	4.2

data points available, was observed between μDMSP in the PAR+UV incubations and Chl *a* concentration (Fig. 5B). The daily rates of μDMSP were consistently higher than μPOC among the different phytoplankton communities, with μPOC on average 20% ± 4% of μDMSP for all six comparable experiments and both treatment incubations.

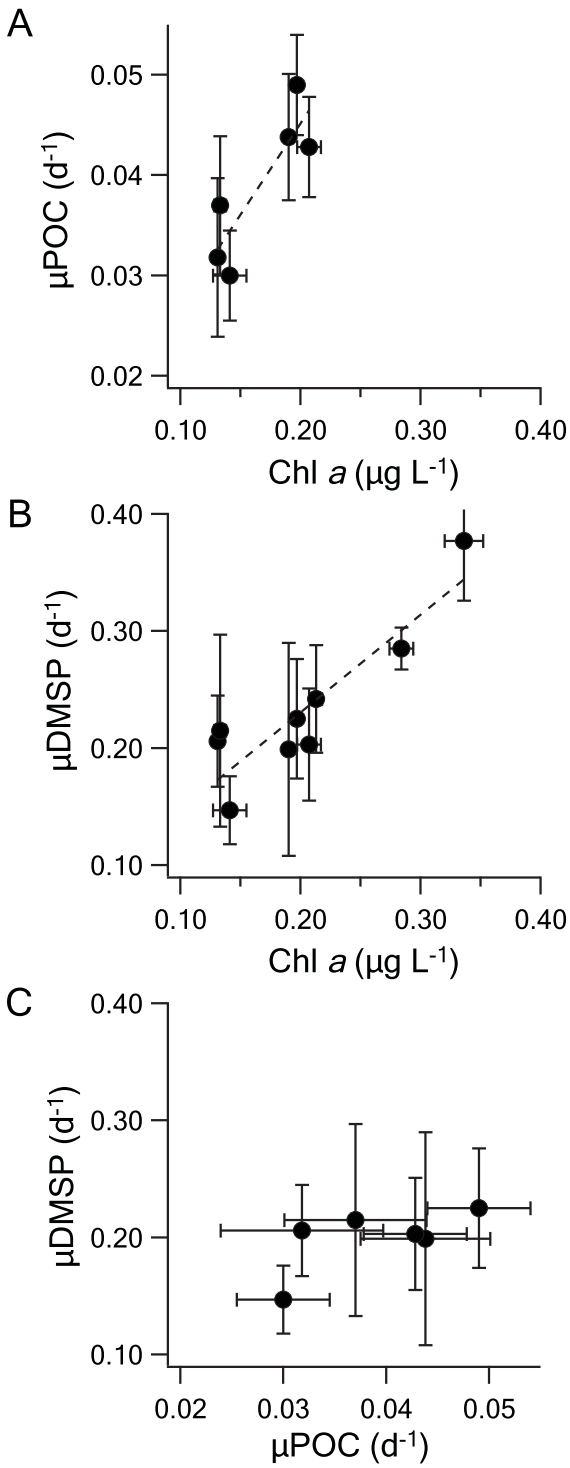

Fig. 5. Relationship between: (**A**) daily POC synthesis (μPOC) and Chl *a* concentration, values for the linear regression are: $y = 0.18x + 0.009$, $r^2 = 0.75$, p of the F statistic = 0.029; (**B**) daily DMSP synthesis (μDMSP) and Chl *a*, values for the linear regression are: $y = 0.84x + 0.063$, $r^2 = 0.79$, p of the F statistic = 0.0012; and (**C**) μDMSP and μPOC, the linear regression is not significant, p of the F statistic = 0.15. Error bars are the propagated SD for μDMSP and μPOC and the range for Chl *a*.

Irradiance dependence of synthesis rates

Comparison between μDMSP and μPOC and the influence of PAR-UV vs. PAR+UV treatments was investigated through photosynthesis vs. irradiance curves (P vs. E) (Fig. 6; Table 4). The relatively short incubation time intervals over the changing diel pattern of irradiance were used to generate light response curves for μDMSP and μPOC by combining data from all experiments. To avoid the influence of light history on photosynthetic physiology, this analysis is restricted to morning and midday incubation time intervals, prior to the point of maximum photoinhibition (Fig. 3).

At both light-limiting and saturated light levels, μPOC was considerably lower than μDMSP (Fig. 6), reflecting the higher daily rates of μDMSP than μPOC, described earlier. At light-limited irradiance the maximum light utilization coefficient α, was fivefold to sevenfold higher for μDMSP compared to μPOC (Table 4). The P vs. E fit indicates that PAR saturation of μDMSP (E_k) occurs at 184 ± 11 μmol photons m^{-2} s^{-1}, which was slightly higher for μPOC at 233 ± 19 μmol photons m^{-2} s^{-1} (Fig. 6; Table 4).

Separate P vs. E curves for PAR-UV and PAR+UV incubations illustrate substantial UVR-mediated inhibition of μDMSP and μPOC (Fig. 6). From the difference between P vs. E relationships for PAR-UV and PAR+UV, the UVR-dependent proportional inhibition of μDMSP was established. During the middle of the day, natural levels of UVR averaging ≥ 40 μmol photon m^{-2} s^{-1} (PAR = 890 μmol photon m^{-2} s^{-1}) resulted in approximately 60% inhibition of μDMSP. A similar inhibition of approximately 55% occurred in μPOC.

Response to photoinhibition of DMSP synthesis vs. NPQ capacity

To examine whether DMSP metabolism responded to short-term photooxidative stress, we compared it to that of a recognized photoprotective mechanism, the xanthophyll cycle. Over the course of the $\sim$ 12 h incubations, the pool size of DMSPt increased by on average ($\pm$ SD) $5\% \pm 12\%$ in the nine experiments, with no significant difference (paired T-test, $p = 0.35$, two-tailed, $n = 9$) between PAR+UV and PAR-UV treatments. Dissolved DMS concentrations showed on average, a $16\% \pm 13\%$ increase during the incubations and were also not significantly different between PAR+UV and PAR-UV treatments (paired T-test, $p = 0.11$, two-tailed, $n = 8$). In contrast, phytoplankton increased their capacity for NPQ in response to increasing irradiance during the day by de novo synthesis of xanthophyll pigments, evident as 60–200% increases in Dd + Dt over the first $\sim$ 6 h of the incubations; considerably larger than changes in DMSP and DMS pools. The proportional increase in Dd + Dt was significantly higher in PAR+UV (average 160%) compared to PAR-UV treatments (average 110%) (paired T-test, $p = 0.006$, $n = 8$). Prior to the point of maximum photoinhibition,

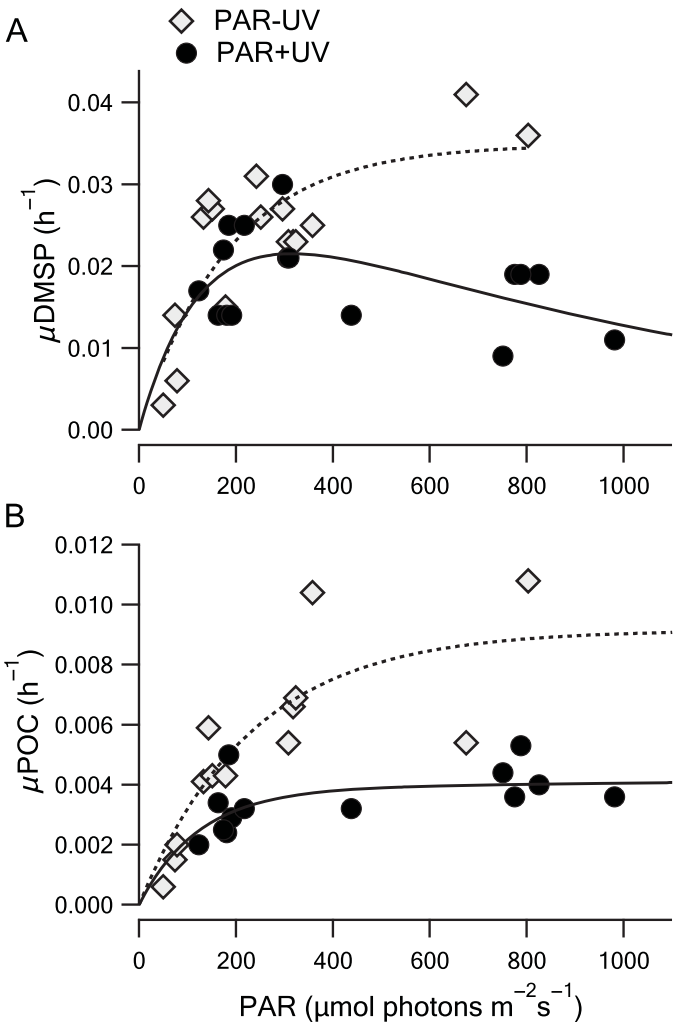

Fig. 6. Irradiance dependence of (**A**) DMSP synthesis (μDMSP), and (**B**) inorganic carbon fixation (μPOC) in phytoplankton communities of the northeastern Tropical Atlantic. The figures are compiled from experiments on different dates and locations (Fig. 1; Table 1). Phytoplankton were incubated in parallel under two different light regimes: PAR+UV and PAR-UV. Data points represent μDMSP or μPOC vs. the average PAR over the duration of each time interval during on-deck incubations. Data is restricted to the time intervals prior to the point of maximum photoinhibition (Fig. 3) in order to avoid the influence of light history on physiology. Coefficients and significance of the P vs. E relationships for μDMSP and μPOC are shown in Table 4.

specific rates of net Dd + Dt synthesis ranged from 0.08 h^{-1} to 0.18 h^{-1} and 0.11 h^{-1} to 0.20 h^{-1} in PAR-UV and PAR+UV treatments, respectively. In contrast to Dd + Dt, Chl *a* concentrations changed by on average, only 3% ± 9% over the first ~ 6 h of the incubations, with no significant difference between treatments. As a result of the preferential synthesis of xanthophyll pigments, the ratios of Dd + Dt : Chl *a* increased on average by 2.5-fold and 2.1-fold and were significantly different (paired *T*-test, $p = 0.38$, two-tailed, $n = 8$) over the first ~ 6 h of the incubations in PAR+UV and PAR-UV treatments, respectively.

When the difference in DMSP production between PAR+UV and PAR-UV treatments was compared to the difference in the NPiR, higher NPiR was associated with a decrease in DMSP production (Fig. 7A). In contrast, higher NPiR was associated with elevated production of Dd + Dt in PAR+UV treatments compared to PAR-UV treatments (Fig. 7B). Higher irradiance, including exposure to UVR, increased the rate of photoinhibition, depressed the rate of DMSP synthesis, and stimulated the rate of synthesis of xanthophyll-cycle pigments.

Discussion

This study presents some of the very few direct measurements of DMSP synthesis rates in natural planktonic communities. These measurements allow us to address several aspects of the physiological basis of DMSP production and provide new insights into the extent of primary production invested in production of this important single compound and the extent to which natural phytoplankton alter that resource allocation on a diel basis. The results presented are from a variety of oceanic locations with phytoplankton communities that had chlorophyll concentrations ranging from 0.13 μg L^{-1} in the central Atlantic to 0.34 μg L^{-1} close to the islands of Cape Verde, and DMSPt : Chl *a* ratios ranging from 38 nmol μg^{-1} to 93 nmol μg^{-1}. Although similar experiments could have been carried out on single strains of microalgae under more controlled conditions in the laboratory, the results from this study are more representative of the response of tropical and subtropical communities in their natural environment.

DMSP synthesis among natural communities

A subset of species that make up natural phytoplankton communities synthesize DMSP; as a result, values of μDMSP are a function of the combination of their varied specific growth rates, relative contributions to the total DMSP pool, and the rate of intracellular turnover of DMSP. Although carbon : Chl *a* ratios and therefore DMSP : Chl *a*, can vary in relation to light levels and photoacclimation, the almost threefold difference in DMSPt : Chl *a* ratio between stations indicates that DMSP-producing phytoplankton made-up a variable component of the phytoplankton biomass in the present study. Despite this, the strong correlation between μDMSP and Chl *a* (Fig. 5) suggests DMSP synthesis is closely coupled to photosynthesis. This assumes Chl *a* concentrations are an approximate index of the extent of light absorption by the respective phytoplankton communities; an assumption supported by the significant relationship between μPOC and Chl *a* (Fig. 5). Whether the observed relationship between μDMSP synthesis and Chl a, and by proxy community photosynthesis, extends beyond the region and time of the present study remains to be established. How closely coupled μDMSP is to photosynthesis is discussed further in the following sections.

Table 4. Irradiance dependence of DMSP synthesis (μDMSP) and inorganic carbon fixation (μPOC) shown in Fig. 6. The P vs. E relationships were calculated as: $\mu = \mu s$ *(1 – exp[$-\alpha$ * PAR/Ps]) * exp($-\beta$ * PAR/Ps) (Platt et al. 1980). Where Ps represents the light-saturated maximum μDMSP or μPOC; α is the maximum light utilization coefficient; β is the photoinhibition parameter; E_k is the light saturation index (= Ps/α); *p* the level of significance (one way ANOVA) between observed and predicted values; and *n* is the number of observations.

	μs ($\times 10^{-3}$) (h^{-1})	α ($\times 10^{-5}$) ([μ h^{-1}] [μmol m^{-2} s^{-1}]$^{-1}$)	β ($\times 10^{-5}$) ([μ h^{-1}] [μmol m^{-2} s^{-1}]$^{-1}$)	E_k (μmol m^{-2} s^{-1})	Significance *p* (*n*)
A. μDMSP					
PAR-UV	35 ± 4	19 ± 4	0.0	184 ± 11	0.0002 (16)
PAR+UV	34 ± 23	22 ± 9	3 ± 5	155 ± 97	0.50 (16)
B. μPOC					
PAR-UV	9.2 ± 1.6	3.9 ± 0.9	0.0	233 ± 19	0.0003 (13)
PAR+UV	3.9 ± 2.2	3.2 ± 1.7	−0.021 ± 0.25	123 ± 74	0.031 (13)

Several studies have now been carried out that directly quantified DMSP synthesis using the stable-isotope approach of Stefels et al. (2009), allowing comparison between a small number of regions and communities. In the northeastern Tropical Atlantic, μDMSP varied from 0.15 d^{-1} to 0.38 d^{-1}, in the full spectrum PAR+UV incubation experiments (Table 3). The differences between stations may be partly explained by light levels that varied from 44% to 96% of the surface irradiance (Fig. 2). These values of μDMSP are generally higher than comparable measurements that averaged 0.14 d^{-1} in four experiments carried out in the low Chl *a* (0.042 μg L^{-1} to 0.064 μg L^{-1}) but high DMSPp : Chl *a* (average 136 nmol μg^{-1}) waters of the Sargasso Sea (Stefels et al. 2009). A larger variation in μDMSP of 0.25–0.74 d^{-1} was observed between phytoplankton communities sampled in the summer from four locations in the shelf seas around the British Isles, when incubated under consistent light levels (Hopkins and Archer 2014). These communities varied 10-fold in Chl *a* concentration (0.3–3.5 μg L^{-1}) and between 30 nmol μg^{-1} and 150 nmol μg^{-1} in DMSPt : Chl *a* ratio. In a separate large pelagic mesocosm experiment in Arctic waters, initial rates of μDMSP were 0.20–0.25 d^{-1} and showed similar temporal trends to carbon fixation during the month-long experiment, with nano-eukaryote phytoplankton, particularly dinoflagellates, dominating the DMSP production (Archer et al. 2013). In incubation experiments with under-ice algal communities, in situ conditions resulted in μDMSP rates of 0.08–0.2 d^{-1}, possibly depending on community composition and nutrient status (Galindo et al. 2016). Unsurprisingly, large regional variations in μDMSP are apparent in these studies but understanding how this variability is linked to photosynthetic carbon fixation may help in developing spatially and temporally broader models of DMSP production.

The direct measurements of μDMSP and μPOC provide an indication of the allocation of photosynthetic resources to DMSP production by natural communities. In the northeastern Tropical Atlantic, phytoplankton communities invested between 4.2% and 9.7% of carbon fixation in DMSP production during daylight in the near-surface environment of the experimental incubations (Table 3). Similar levels of allocation of fixed carbon to DMSP production have been observed using less direct approaches. For instance, in an *E. huxleyi* bloom in the northern North Sea, DMSP production estimated from dilution experiments averaged 4.8–9.1% of carbon fixation determined from ^{14}C-incubations (Archer et al. 2001). An approximation of the global oceanic DMSP production has been derived from satellite-based estimates of chlorophyll converted to DMSPt concentrations, to which a fixed turnover rate of DMSPt was applied (Galí et al. 2015). This analysis provided an estimate of 3.8 Pg C yr^{-1} invested in DMSP production by phytoplankton in the upper ocean that was equivalent to between 5% and 9% of estimates of gross carbon production. The similarity between this satellite-derived approximation of photosynthesis invested in DMSP and the direct measurements from the northeastern Tropical Atlantic and northern North Sea emphasizes the importance of DMSP as a component of carbon biogeochemistry. In contrast, a much lower percentage allocation to DMSP production was observed during the mesocosm experiment in Arctic waters; < 1% of carbon fixation was invested in DMSP synthesis, when ^{13}C-based μDMSP rates are compared to ^{14}C-based estimates of carbon fixation (Archer et al. 2013). A similar, relatively low proportion of 1.5% of water-column integrated carbon fixation can be calculated from rates of $^{35}SO_4^{2-}$ incorporation into non-protein reduced-sulfur products, assumed to be DMSP, relative to ^{14}C-based estimates of carbon fixation (Bates et al. 1994). What dictates this order-of-magnitude difference in resource allocation is still unclear but understanding the physiological roles of DMSP is likely to hold the answers.

DMSP synthesis and photoinhibition

Comparisons of the P vs. E relationships for DMSP synthesis and carbon fixation, allow the physiological basis of DMSP production to be explored. If DMSP production is regulated in the short term as a photoprotective antioxidant, we expected DMSP synthesis to be elevated at high light intensities including UVR, compared to photosynthetic carbon fixation. The irradiance dependence for the specific rates of inorganic carbon

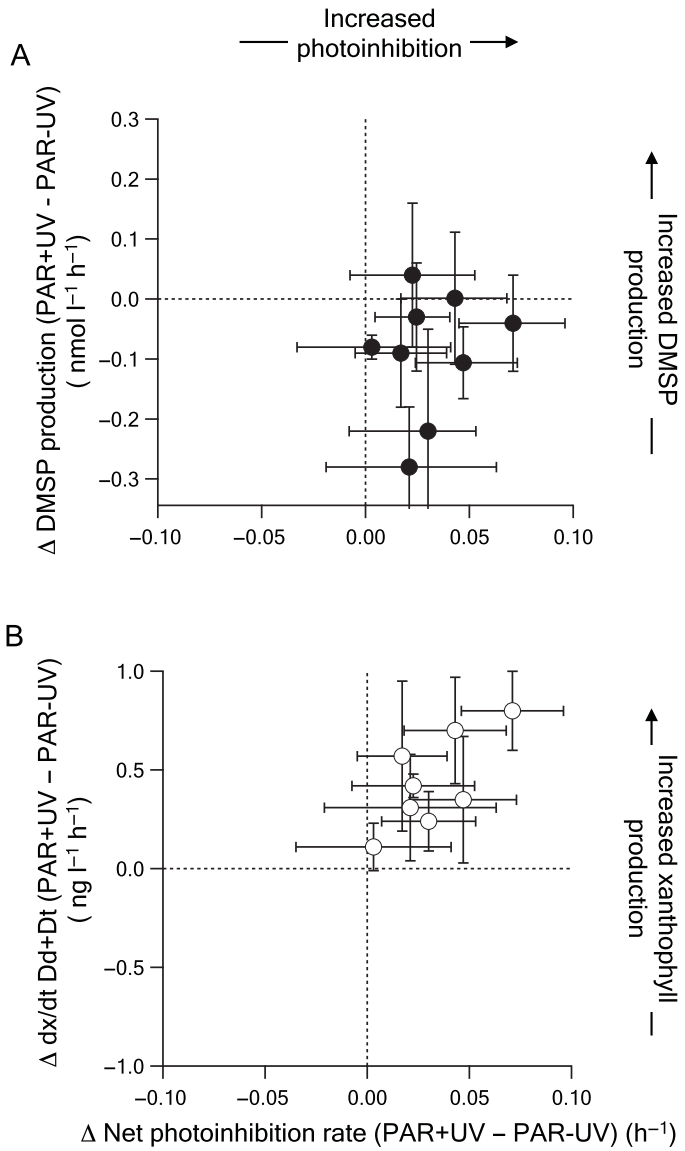

Fig. 7. Physiological response to irradiance-mediated photoinhibition in phytoplankton communities of the northeastern Tropical Atlantic. (**A**) Difference in DMSP production (Δ DMSP production) related to differences in photoinhibition (Δ net photoinhibition rate) between incubation treatments (PAR+UV – PAR-UV). DMSP production was calculated from μDMSP and initial DMSP concentration. (**B**) Difference in xanthophyll pigment production (Δ d*x*/d*t* Dd + Dt) and Δ net photoinhibition rate between incubation treatments (PAR+UV – PAR-UV). Δ DMSP production and Δ d*x*/d*t* Dd + Dt were calculated over the time intervals prior to the point of maximum photoinhibition (Fig. 3). Error bars are the propagated SD.

fixation into particulate organic carbon (μPOC vs. E) determined in parallel incubations, yielded considerably lower μPOC than μDMSP at all irradiances, both light-limiting and light saturating (Fig. 6; Table 3). This is expected since a substantial proportion of POC may comprise detrital and heterotrophic biomass, while most DMSP is contained in phytoplankton. This does not affect comparison of E_k; which was slightly higher for μPOC at 233 ± 19 μmol photons m^{-2} s^{-1} vs. 184 ± 11 μmol photons m^{-2} s^{-1} for μDMSP, in PAR-UV incubations (Fig. 6; Table 4). The E_k value for μPOC is consistent with an average E_k of 238 μmol photon m^{-2} s^{-1} for carbon fixation compiled from multiple studies in the tropical and Sub-tropical Atlantic and Pacific (Uitz et al. 2008), and comparable to an E_k of 228 ± 16 μmol photons m^{-2} s^{-1} for photosynthetic electron transport measured in the northern Tropical Atlantic (Suggett et al. 2006); both studies excluded the influence of UVR in their measurements. The comparable E_k values for μDMSP and μPOC indicate that DMSP synthesis is closely coupled to carbon fixation rather than being stimulated at high irradiance, as would be expected if regulated as a photoprotective antioxidant. This does not exclude the potential intracellular reaction of DMSP and its breakdown products with reactive oxygen species (ROS) (Sunda et al. 2002), but it does indicate that regulation of DMSP production on a diel timescale is not linked to photooxidative stress in the natural communities that we examined.

In the short-term light-manipulation experiments of the present study, where changes in taxonomic composition are considered not to be a factor, μDMSP is also a function of any physiological response that alters the allocation of photosynthetic production to DMSP between treatments. To further examine whether DMSP production responds to short-term photooxidative stress, we compared it to that of a recognized photoprotective mechanism. To minimize ROS production, many photosynthetic organisms dissipate excess excitation energy in the form of heat (NPQ) through the xanthophyll cycle. In members of the Bacillariophyceae, Xanthophyceae, Haptophyceae, and Dinophyceae microalgal classes, rapid photoregulatory NPQ responses stimulated by raised proton (H^+) concentration in the thylakoid lumen, involve the enzymatic de-epoxidation of Dd to Dt. (Goss and Jakob 2010). A slower photoacclimatory response to high light and photoinhibition, over hours or days, involves increased de novo synthesis of the xanthophyll pigment pool (van de Poll and Buma 2009). This photoacclimatory response was compared to production rates of DMSP. In the incubations of this study, the phytoplankton communities exhibited increased photoinhibition during the middle of the day (Fig. 3). This is typical of phytoplankton populations in low nutrient, low biomass open ocean environments (Mackey et al. 2008). The levels of photoinhibition were typically higher in PAR+UV than in PAR-UV treatments. This photoinhibition most likely stemmed from both direct photo-damage of the reaction centers of PSII triggered by singlet oxygen production and the inhibition of protein synthesis and PSII repair through the activity of elevated concentrations of ROS (Krieger-Liszkay et al. 2008, Takahashi and Murata 2008, Roach and Krieger-Liszkay 2014). Contrary to expectations, we found that in response to increased photooxidative stress in PAR+UV treatments DMSP production was generally inhibited compared to PAR-UV treatments (Fig. 7). In contrast, phytoplankton increased their capacity for NPQ

in response to increasing irradiance during the day by de novo synthesis of xanthophyll pigments, evident as 60–200% increases in Dd + Dt; considerably larger than changes in DMSP and DMS pools. Moreover, and in contrast to DMSP production, increased rates of photoinhibition in PAR+UV treatments were associated with net production of xanthophyll pigments of between 10% and 100% above PAR-UV incubations (Fig. 7). This up-regulation of NPQ capacity can most likely be assigned to the main DMSP-producing components of the phytoplankton, as the Haptophyceae and Dinophyceae which were present in these waters, are typically high DMSP-producers and specifically employ the Dd + Dt form of xanthophyll cycle. High ratios of the pigment markers hexanoyloxyfucoxanthin to fucoxanthin (data not shown) of 3–7, supports the presence of Haptophyceae in the waters used for the experiments. Unlike the xanthophyll cycle pigments, DMSP production appears not to be regulated in the short term by the necessity to control increasing photooxidative stress as irradiance increases during the day.

From the difference between P vs. E relationships for PAR-UV and PAR+UV an UVR-dependent, proportional inhibition of μPOC and μDMSP can be established. During the middle of the day, natural levels of UVR averaging ≥ 40 μmol photon m^{-2} s^{-1} (PAR = 890 μmol photon m^{-2} s^{-1}) resulted in approximately 60% inhibition of μDMSP in the near-surface environment of the incubations. A similar inhibition of approximately 55% occurred in μPOC (Fig. 6). The single simulated depth of the incubations in the present study does not take into account the dynamic light environment that a vertically mixed particle in the surface ocean might encounter, although the incubations do accommodate the physiological adjustments that phytoplankton make to the diel patterns of irradiance. Photoinhibition due to high light and UVR can be enhanced or depressed due to vertical mixing, depending on a combination of the depth of the mixing layer, rates of mixing and the extent of light attenuation (Neale et al. 1998, MacIntyre et al. 2000). The response to high light and UVR and levels of photoinhibition observed in the incubations may have been influenced by the light history experienced by phytoplankton isolated from the dynamic mixing regime of the considerably deeper mixed layer (Table 2). The incubations of the PAR+UV treatments approximated the light environment of a particle that remained in the top 10 m of the water column during the daylight period (Table 2). To minimize light history affects, interpretation of the physiological responses were limited to approximately the first 6 h of the day in each experiment (Figs. 6, 7; Table 4).

The levels of UVR-induced inhibition observed in the present study are consistent with the extent of inhibition of carbon fixation previously observed in low-nutrient tropical and sub-tropical waters. For instance, in tropical oceanic waters of the South China Sea, rates of carbon fixation measured over 6 h during the middle of the day were inhibited by 20% to 30% by a combination of UVA and UVB (Li et al. 2011). Inhibition by 16–55% of hourly rates of carbon fixation due to a combination of UVA and UVB was observed in the shallow waters (1–8 m) of a tropical coral reef lagoon (Conan et al. 2008). In short-term incubations (200 min) of water from the oligotrophic southeastern Indian Ocean, differences in P vs. E relationships between UV-opaque and UV-transparent incubations illustrated up to 49% inhibition of carbon fixation due to UVR-exposure at the highest levels of irradiance (Fuentes-Lema et al. 2015). This combination of studies indicate that resource allocation to photoprotective mechanisms by phytoplankton adapted to the high-light environments of the tropical and subtropical ocean, is finely balanced and does not prevent UVR-induced photoinhibition during the middle of the day in near-surface waters. How and why this balance varies between different components of phytoplankton communities largely remains to be explored.

The close coupling between μDMSP and μPOC observed in this study contrasts with the response of single strains of the prymnesiophyte *E. huxleyi* in laboratory experiments. In general, exposure to high light and UVR stimulate the cell-specific production of DMSP in *E. huxleyi* cultures suggesting that UVR induces increased synthesis of DMSP relative to carbon fixation in *E. huxleyi*. However, variations in the response were associated with light levels to which the cells were acclimated, different strains, and duration and intensity of the UVR exposure (Sunda et al. 2002; van Rijssel and Buma 2002, Slezak and Herndl 2003, Archer et al. 2010, Darroch et al. 2015). Moreover, these studies measured changes in DMSP concentrations rather than μDMSP rates and therefore, may not be fully comparable with our data. A challenging aspect of such laboratory studies is to incorporate the capacity of cells to acclimate to diel and mixing-driven variability in irradiance and high levels of UVR to which they are exposed in nature.

A common feature of the response to UVR among strains of *E. huxleyi* is increased release of DMSP to the dissolved phase (Archer et al. 2010, Darroch et al. 2015) and this was not examined in this study. Enhanced production of dissolved organic carbon (DOC) has been quantified in natural oceanic communities when exposed to enhanced levels of UVR (Fuentes-Lema et al. 2015). If DMSP is released from cells exposed to UVR in common with other components of the DOC, the resulting increased dissolved DMSP availability potentially boosts DMS production. Several studies conducted in high-light oceanic waters have shown enhanced DMS production in incubations exposed to near surface levels of PAR and UVR (Toole et al. 2006, Galí et al. 2013). Although, these studies also showed that UVR enhancement of DMS production is to some extent balanced by increased rates of DMS photolysis. One possible but challenging means to examine whether UVR-induced release of DMSP drives DMS production would be extension of the tracer approach and experimental design used in this study to directly track the release of intracellular DMSP to the dissolved phase and to DMS production. Introducing direct measurements of rates of DMSP synthesis and intracellular turnover to

recently isolated, single strain, culture based physiological studies on appropriate tropical phytoplankton taxa may be the most tractable approach initially.

Conclusion

In conclusion, several lines of evidence from this study indicate that on a diel basis DMSP synthesis is not enhanced when tropical and subtropical phytoplankton communities are exposed to natural high light levels that cause reversible photoxidative stress. Firstly, P vs. E relationships based on μDMSP and μPOC and irradiance measured over discrete time intervals during the course of the day, showed similar values of PAR saturation (E_k). This demonstrates that DMSP synthesis was not upregulated at high light levels and was closely coupled to carbon fixation. Second, enhanced photooxidative stress due to UVR exposure clearly stimulated de novo synthesis of photoprotective xanthophyll-cycle pigments (Dd + Dt), above levels induced by high PAR alone. In contrast, DMSP production was inhibited by exposure to UVR. Synthesis of DMSP does not appear to be involved in the acclimatory response of phytoplankton to changing light levels including UVR exposure on the timescale of vertical mixing or diel variation. Although both eukaryotic and prokaryotic phytoplankton are known to possess a suite of photoprotective mechanisms, community level carbon fixation and DMSP synthesis appear to be inhibited by UVR exposure during the middle of the day in near-surface waters of the tropical ocean. Strong evidence that DMSP synthesis is associated with an antioxidant role (Sunda et al. 2002) or acts as an overflow product of excess photosynthetic production (Stefels 2000) in high-light, oceanic environments of the tropical and subtropical oceans, remains to be established.

References

Archer, S. D., C. E. Widdicombe, G. A. Tarran, A. P. Rees, and P. H. Burkill. 2001. Production and turnover of particulate dimethylsulphoniopropionate during a coccolithophore bloom in the northern North Sea. Aquat. Microb. Ecol. **24**: 225–241. doi:10.3354/ame024225

Archer, S. D., M. Ragni, R. Webster, R. L. Airs, and R. J. Geider. 2010. Dimethyl sulfoniopropionate and dimethyl sulfide production in response to photoinhibition in *Emiliania huxleyi*. Limnol. Oceanogr. **55**: 1579–1589. doi:10.4319/lo.2010.55.4.1579

Archer, S. D., S. A. Kimmance, J. A. Stephens, F. E. Hopkins, R. Bellerby, K. G. Schulz, J. Piontek, and A. Engel. 2013. Contrasting responses of DMS and DMSP to ocean acidification in Arctic waters. Biogeosciences **10**: 1893–1908. doi:10.5194/bg-10-1893-2013

Barlow, R. G., D. G. Cummings, and S. W. Gibb. 1997. Improved resolution of mono-and divinyl chlorophylls a and b and zeaxanthin and lutein in phytoplankton extracts using reverse phase C-8 HPLC. Mar. Ecol. Prog. Ser. **161**: 303–307. doi:10.3354/meps161303

Bates, T. S., R. P. Kiene, G. V. Wolfe, P. A. Matrai, F. P. Chavez, K. R. Buck, B. W. Blomquist, and R. L. Cuhel. 1994. The cycling of sulfur in surface seawater of the northeast Pacific. J. Geophys. Res. Oceans **99**: 7835–7843. doi:10.1029/93JC02782

Cainey, J. M., H. Sievering, and G. P. Ayers. 2008. Where to now? A synthesis of current views of the CLAW hypothesis. Environ. Chem. **4**: 406–409. doi:10.1071/EN07082

Challenger, F., and M. I. Simpson. 1948. Studies on biological methylation. Part XII. A precursor of the dimethyl sulphide evolved by *Polysiphonia fastigiata*. Dimethyl-2-carboxyethylsulphonium hydroxide and its salts. J. Chem. Soc. **320**: 1591–1597. doi:10.1039/jr9480001591

Charlson, R. J., J. E. Lovelock, M. O. Andreae, and S. G. Warren. 1987. Oceanic phytoplankton, atmospheric sulphur, cloud albedo and climate. Nature **326**: 655–661. doi:10.1038/326655a0

Chen, T., and M. Jang. 2012. Secondary organic aerosol formation from photooxidation of a mixture of dimethyl sulfide and isoprene. Atmos. Environ. **46**: 271–278. doi:10.1016/j.atmosenv.2011.09.082

Conan, P., F. Joux, J. P. Torréton, M. Pujo-Pay, T. Douki, E. Rochelle-Newall, and X. Mari. 2008. Effect of solar ultraviolet radiation on bacterio-and phytoplankton activity in a large coral reef lagoon (southwest New Caledonia). Aquat. Microb. Ecol. **52**: 83–98. doi:10.3354/ame01204

Dacey, J. W., and S. G. Wakeham. 1986. Oceanic dimethylsulfide: Production during zooplankton grazing on phytoplankton. Science **233**: 1314–1316. doi:10.1126/science.233.4770.1314

Darroch, L. J., and others. 2015. Effect of short-term light- and UV-stress on DMSP, DMS, and DMSP lyase activity in *Emiliania huxleyi*. Aquat. Microb. Ecol. **74**: 173–185. doi:10.3354/ame01735

Fuentes-Lema, A., C. Sobrino, N. González, M. Estrada, and P. J. Neale. 2015. Effect of solar UVR on the production of particulate and dissolved organic carbon from phytoplankton assemblages in the Indian Ocean. Mar. Ecol. Prog. Ser. **535**: 47–61. doi:10.3354/meps11414

Galí, M., R. Simó, G. L. Pérez, C. Ruiz-González, H. Sarmento, S. J. Royer, A. Fuentes-Lema, and J. M. Gasol. 2013. Differential response of planktonic primary, bacterial, and dimethylsulfide production rates to static vs. dynamic light exposure in upper mixed-layer summer sea waters. Biogeosciences **10**: 7983–7998. doi:10.5194/bgd-10-8851-2013

Galí, M., and R. Simó. 2015. A meta-analysis of oceanic DMS and DMSP cycling processes: Disentangling the summer paradox. Global Biogeochem. Cycles **29**: 496–515. doi:10.1002/2014GB004940

Galí, M. E., M. Devred, S. J. Levasseur, M. Royer, and M. Babin. 2015. A remote sensing algorithm for planktonic dimethylsulfoniopropionate (DMSP) and an analysis of global patterns. Remote Sens. Environ. **171**: 171–184. doi:10.1016/j.rse.2015.10.012

Galindo, V., and others. 2016. Contrasted sensitivity of DMSP production to high light exposure in two Arctic

under-ice blooms. J. Exp. Mar. Biol. Ecol. **475**: 38–48. doi: 10.1016/j.jembe.2015.11.009

Goss, R., and T. Jakob. 2010. Regulation and function of xanthophyll cycle-dependent photoprotection in algae. Photosyn. Res. **106**: 103–122. doi:10.1007/s11120-010-9536-x

Halsey, K. H., and B. M. Jones. 2015. Phytoplankton strategies for photosynthetic energy allocation. Ann. Rev. Mar. Sci. **7**: 265–297. doi:10.1146/annurev-marine-010814-015813

Hopkins, F. E., and S. D. Archer. 2014. Consistent increase in dimethyl sulfide (DMS) in response to high CO_2 in five shipboard bioassays from contrasting NW European waters. Biogeosciences **11**: 4925–4940. doi:10.5194/bg-11-4925-2014

Ishida, Y. 1996. 30 years of research on dimethylsulfoniopriopionate, p. 1–12. *In* M. D. Keller, R. P. Kiene, G. O. Kirst, and P. T. Visscher [eds.], Biological and environmental chemistry of DMSP and related sulfonium compounds. Springer.

Jeffrey, S. W., R. F. C. Mantoura, and T. Bjørnland. 1997. Data for the identification of 47 key phytoplankton pigments. Phytoplankton pigments in oceanography: guidelines to modern methods. UNESCO, Paris, pp 449–559.

Johnson, M. T., and T. G. Bell. 2008. Coupling between dimethylsulfide emissions and the ocean–atmosphere exchange of ammonia. Env. Chem. **5**: 259–267. doi:10.1071/EN08030

Kates, M., and B. E. Volcani. 1996. Biosynthetic pathways for phosphatidylsulfocholine, the sulfonium analogue of phosphatidylcholine, in diatoms, p. 109–119. *In* M. D. Keller, R. P. Kiene, G. O. Kirst, and P. T. Visscher [eds.], Biological and environmental chemistry of DMSP and related sulfonium compounds. Springer.

Keller, M. D., W. K. Bellows, and R. R. L. Guillard. 1989. Dimethyl sulfide production in marine phytoplankton, p. 183–200. In E. S. Saltzman and W. J. Cooper [eds.], Biogenic sulfur in the environment. American Chemical Society.

Kiene, R. P., and D. Slezak. 2006. Low dissolved DMSP concentrations in seawater revealed by small-volume gravity filtration and dialysis sampling. Limnol. Oceanogr.: Methods **4**: 80–95. doi:10.4319/lom.2006.4.80

Kirkby, J., and others. 2011. Role of sulphuric acid, ammonia and galactic cosmic rays in atmospheric aerosol nucleation. Nature **476**: 429–433. doi:10.1038/nature10343

Kolber, Z. S., O. Prášil, and P. G. Falkowski. 1998. Measurements of variable chlorophyll fluorescence using fast repetition rate techniques: Defining methodology and experimental protocols. Biochim. Biophys. Acta **1367**: 88–106. doi:10.1016/S0005-2728(98)00135-2

Krieger-Liszkay, A., C. Fufezan, and A. Trebst. 2008. Singlet oxygen production in photosystem II and related protection mechanism. Photosyn. Res. **98**: 551–564. doi: 10.1007/s11120-008-9349-3

Li, G., K. Gao, and G. Gao. 2011. Differential impacts of solar UV radiation on photosynthetic carbon fixation from the coastal to offshore surface waters in the South China Sea. Photochem. Photobiol. **87**: 329–334. doi: 10.1111/j.1751-1097.2010.00862.x

Lana, A., and others. 2011. An updated climatology of surface dimethlysulfide concentrations and emission fluxes in the global ocean. Global Biogeochem. Cycles **25**: GB1004. doi:10.1029/2010GB003850

Le Clainche, Y., and others. 2010. A first appraisal of prognostic ocean DMS models and prospects for their use in climate models. Global Biogeochem. Cycles **24**: GB3021. doi:10.1029/2009GB003721

Lyon, B. R., P. A. Lee, J. M. Bennett, G. R. DiTullio, and M. G. Janech. 2011. Proteomic analysis of a sea-ice diatom: Salinity acclimation provides new insight into the dimethylsulfoniopropionate production pathway. Plant Physiol. **157**: 1926–1941. doi:10.1104/pp.111.185025

MacIntyre, H. L., T. M. Kana, and R. J. Geider. 2000. The effect of water motion on short-term rates of photosynthesis by marine phytoplankton. Trends Plant Sci. **5**: 12–17. doi:10.1016/S1360-1385(99)01504-6

Mackey, K. R., A. Paytan, A. R. Grossman, and S. Bailey. 2008. A photosynthetic strategy for coping in a high-light, low-nutrient environment. Limnol. Oceanogr. **53**: 900–913. doi:10.4319/lo.2008.53.3.0900

Mahajan, A. S., S. Fadnavis, M. A. Thomas, L. Pozzoli, S. Gupta, S. J. Royer, and R. Simó. 2015. Quantifying the impacts of an updated global dimethyl sulfide climatology on cloud microphysics and aerosol radiative forcing. J. Geophys. Res.: Atmos. **120**: 2524–2536. doi:10.1002/2014JD022687

Neale, P. J., J. J. Cullen, and R. F. Davis. 1998. Inhibition of marine photosynthesis by ultraviolet radiation: Variable sensitivity of phytoplankton in the Weddell-Scotia Confluence during the austral spring. Limnol. Oceanogr. **43**: 433–448. doi:10.4319/lo.1998.43.3.0433

Platt, T., C. L. Gallegos, and W. G. Harrison. 1980. Photoinhibition of photosynthesis in natural assemblages of marine phytoplankton. J. Mar. Syst. **38**: 103–111.

Polimene, L., S. D. Archer, M. Butenschön, and J. I. Allen. 2012. A mechanistic explanation of the Sargasso Sea DMS "summer paradox". Biogeochemistry **110**: 243–255. doi: 10.1007/s10533-011-9674-z

Quinn, P. K., and T. S. Bates. 2011. The case against climate regulation via oceanic phytoplankton sulphur emissions. Nature **480**: 51–56. doi:10.1038/nature10580

Ragni, M., R. L. Airs, N. Leonardos, and R. J. Geider. 2008. Photoinhibition of PSII in *Emiliania huxleyi* (Haptophyta) under high light stress: The roles of photoacclimation, photoprotection, and photorepair. J. Phycol. **44**: 670–683. doi:10.1111/j.1529-8817.2008.00524.x

Rinaldi, M., and others. 2010. Primary and secondary organic marine aerosol and oceanic biological activity: Recent results and new perspectives for future studies. Adv. Meteorol. **2010**: 310682. doi:10.1155/2010/310682

Roach, T., and A. Krieger-Liszkay. 2014. Regulation of photosynthetic electron transport and photoinhibition. Curr. Protein Pept. Sci. **15**: 351–362. doi:10.2174/1389203715666140327105143

Schlitzer, R. 2015. Ocean Data View. http://odv.awi.de.

Seymour, J. R., R. Simó, T. Ahmed, and R. Stocker. 2010. Chemoattraction to dimethylsulfoniopropionate throughout the marine microbial food web. Science **329**: 342–345. doi:10.1126/science.1188418

Sipilä, M., and others. 2010. The role of sulfuric acid in atmospheric nucleation. Science **327**: 1243–1246. doi:10.5194/acpd-10-25959-2010

Slezak, D., and G. J. Herndl. 2003. Effects of ultraviolet and visible radiation on the cellular concentrations of dimethylsulfoniopropionate (DMSP) in *Emiliania huxleyi* (strain L). Mar. Ecol. Prog. Ser. **246**: 61–71. doi:10.3354/meps246061

Stefels, J. 2000. Physiological aspects of the production and conversion of DMSP in marine algae and higher plants. J. Sea Res. **43**: 183–197. doi:10.1016/S1385-1101(00)00030-7

Stefels, J., M. Steinke, S. Turner, G. Malin, and S. Belviso. 2007. Environmental constraints on the production and removal of the climatically active gas dimethylsulphide (DMS) and implications for ecosystem modelling. Biogeochemistry **83**: 245–275. doi:10.1007/s10533-007-9091-5

Stefels, J., J. W. H. Dacey, and J. T. M. Elzenga. 2009. In vivo DMSP-biosynthesis measurements using stable-isotope incorporation and proton-transfer-reaction mass spectrometry (PTR-MS). Limnol. Oceanogr.: Methods **7**: 595–611. doi:10.4319/lom.2009.7.595

Suggett, D. J., C. M. Moore, E. Maranon, C. Omachi, R. A. Varela, J. Aiken, and P. M. Holligan. 2006. Photosynthetic electron turnover in the tropical and subtropical Atlantic Ocean. Deep-Sea Res. Part II Top. Stud. Oceanogr. **53**: 1573–1592. doi:10.1016/j.dsr2.2006.05.014

Sunda, W., D. J. Kieber, R. P. Kiene, and S. Huntsman. 2002. An antioxidant function for DMSP and DMS in marine algae. Nature **418**: 317–320. doi:10.1038/nature00851

Takahashi, S., and N. Murata. 2008. How do environmental stresses accelerate photoinhibition? Trends Plant Sci. **13**: 178–182. doi:10.1016/j.tplants.2008.01.005

Tedetti, M., and R. Sempéré. 2006. Penetration of ultraviolet radiation in the marine environment. A review. Photochem. Photobiol. **82**: 389–397. doi:10.1562/2005-11-09-IR-733

Toole, D. A., D. Slezak, R. P. Kiene, D. J. Kieber, and D. A. Siegel. 2006. Effects of solar radiation on dimethylsulfide cycling in the western Atlantic Ocean. Deep-Sea Res. Part I Oceanogr. Res. Pap. **53**: 136–153. doi:10.1016/j.dsr.2005.09.003

Toumi, R. 1994. BrO as a sink for dimethylsulfide in the marine atmosphere. Geophys. Res. Lett. **21**: 117–120. doi:10.1029/93GL03536

Trossat, C., B. Rathinasabapathi, E. A. Weretilnyk, T. L. Shen, Z. H. Huang, D. A. Gage, and A. D. Hanson. 1998. Salinity promotes accumulation of 3-dimethylsulfoniopropionate and its precursor S-methylmethionine in chloroplasts. Plant Physiol. **116**: 165–171. doi:10.1104/pp.116.1.165

Uitz, J., Y. Huot, F. Bruyant, M. Babin, and H. Claustre. 2008. Relating phytoplankton photophysiological properties to community structure on large scales. Limnol. Oceanogr. **53**: 614–630. doi:10.4319/lo.2008.53.2.0614

Vallina, S. M., R. Simó, T. R. Anderson, A. Gabric, R. Cropp, and J. M. Pacheco. 2008. A dynamic model of oceanic sulfur (DMOS) applied to the Sargasso Sea: Simulating the dimethylsulfide (DMS) summer paradox. J. Geophys. Res. **113**: G01009. doi:10.1029/2007JG000415

van de Poll, W. H., and A. G. J. Buma. 2009. Does ultraviolet radiation affect the xanthophyll cycle in marine phytoplankton? Photochem. Photobiol. Sci. **8**: 1295–1301. doi:10.1039/b904501e

van Rijssel, M., and A. G. Buma. 2002. UV radiation induced stress does not affect DMSP synthesis in the marine prymnesiophyte *Emiliania huxleyi*. Aquat. Microb. Ecol. **28**: 167–174. doi:10.3354/ame028167

Vidussi, F., H. Claustre, B. B. Manca, A. Luchetta, and J. C. Marty. 2001. Phytoplankton pigment distribution in relation to upper thermocline circulation in the eastern Mediterranean Sea during winter. J. Geophys. Res. **106**: 19939–19956. doi:10.1029/1999JC000308

Vogt, M., S. M. Vallina, E. T. Buitenhuis, L. Bopp, and C. Le Quere. 2010. Simulating dimethylsulphide seasonality with the Dynamic Green Ocean Model PlankTOM5. J. Geophys. Res. **115**: L06021. doi:10.1029/2009JC005529

Wolfe, G. V., and M. Steinke. 1996. Grazing-activated production of dimethyl sulfide (DMS) by two clones of *Emiliania huxleyi*. Limnol. Oceanogr. **41**: 1151–1160. doi:10.4319/lo.1996.41.6.1151

Woodhouse, M. T., K. S. Carslaw, G. W. Mann, S. M. Vallina, M. Vogt, P. R. Halloran, and O. Boucher. 2010. Low sensitivity of cloud condensation nuclei to changes in the sea-air flux of dimethyl-sulphide. Atmos. Chem. Phys. **10**: 7545–7559. doi:10.5194/acp-10-7545-2010

Zubkov, M. V., and P. H. Burkill. 2006. Syringe pumped high speed flow cytometry of oceanic phytoplankton. Cytometry A **69**: 1010–1019. doi:10.1002/cyto.a.20332

Acknowledgments

We thank two anonymous reviewers for their useful input to the manuscript. The authors would also like to thank the officers and crew of RRS *Discovery* and the principal scientist E. Achterberg for support during research cruise D326. We gratefully acknowledge financial support from the Natural Environment Research Council, United Kingdom (NERC, UK) as part of the Surface Ocean Lower Atmosphere Studies (SOLAS) thematic (NE/C51715X/1 to SDA and RJG), and from the National Science Foundation, United States (NSF project OCE-1316133 to SDA).

Conflict of Interest

None declared.

Submitted 28 January 2017
Revised 05 June 2017
Accepted 12 June 2017

Associate editor: M. Dileep Kumar